

A MODEL-FREE CROSS-COUPLED CONTROL FOR POSITION SYNCHRONIZATION OF MULTI-AXIS MOTIONS: THEORY AND EXPERIMENTS

*Dong Sun, Xiaoyin Shao, Geng Feng

*Department of Manufacturing Engineering and Engineering Management
City University of Hong Kong, 83 Tat Chee Avenue, Kowloon, Hong Kong*

Abstract: In this paper, a model-free cross-coupled controller is proposed for position synchronization of multi-axis motions. The position synchronization error of each axis is defined as the differential position error between this axis and its two adjacent axes, which is then coupled with the position error to form a coupled position error. A PD-type synchronization controller with feedback of this coupled position error has been proven to guarantee asymptotic convergence to zero of both position and synchronization errors in a set-point motion control. A trajectory tracking controller is further developed by adding feedforward control terms and a saturation function to the PD synchronization controller. The proposed method is easy to implement in practice since it is model free and the control gains are not time-varying. Experiments are performed to verify effectiveness of the proposed approach. *Copyright © 2005 IFAC*

Keywords: Cross-Coupling, Synchronization, Multi-axis motion

1. INTRODUCTION

With the ever increasing demand for greater productivity and lower cost, there is tremendous pressure to achieve rapid development with high performance in modern manufacturing. Those manufacturing devices such as surface mounting technology (SMT) machines or Complex Numerical Control (CNC) machine tools are accordingly required to have all machine axes move simultaneously or synchronously for either reducing work-in-progress or complex part machining. Poor synchronization of relevant motion control axes results in diminished dimensional accuracy of the work-piece or even in unusable products.

The existing cross-coupling technology (Koren, *et al.*, 1980; Tomizuha, *et al.*, 1992) provides advantages and opportunities to improve synchronization performance. Recently, the cross-coupling concept was incorporated into adaptive control architecture to solve position synchronization of multiple axes (Sun, 2003). The cross-coupling technology has been used in robotics, such as mobile robot control (Feng, 1993)

and coordination of robot manipulators (Sun and Mills, 2002). The solutions for contour tracking problem can be found in the work by Chiu, *et al.*, (2001) and McNab, *et al.*, (1994). It is noted that most of the proposed synchronous controllers rely on modeling dynamics, while the significant demand in practice is to use the model free control algorithm without heavy computation online. A model free variable-gain cross-coupling controller was introduced for a general class of contours (Koren, *et al.*, 1991), but the effect of a time-varying gain in the cross-coupling controller to system stability and the cross-coupling effect on overall system dynamics are yet to be examined (Chiu, *et al.*, 2001). Another effort to examine the stability and robustness of the cross-coupled control system was reported in the work by Yeh, *et al.*, (1997).

In this paper, a simple model free cross-coupled controller is proposed to stabilize multi-axis motions while synchronizing positions of these axes. Unlike the work by Sun (2003), the synchronization error is defined as the differential position error between each axis and its two adjacent axes, and such synchronization error is linearly coupled with the position error to form a coupled position error. It has been shown that a PD-type synchronization controller with feedback of this coupled position error can guarantee asymptotic convergence to zero of both position and synchronization errors for a

*Corresponding author. Tel: (852) 2788-8405;
Fax: (852) 2788-8423 Email: medsun@cityu.edu.hk

set-point motion control. This controller differs from the standard PD control in that not only the convergence of position errors to zero is guaranteed, but also the relationship amongst position errors of all motion axes is regulated. The feedforward control terms and a saturation function can be further added to the PD-type synchronization controller to solve asymptotic trajectory tracking problem. Compared to the existing synchronous control algorithms, the proposed method is very simple since it is model free and the control gains are not time-varying. Experimental results demonstrate the effectiveness of the proposed approaches.

2. POSITION SYNCHRONIZATION ERRORS

Consider the dynamics of a motion system with n axes in the matrix format:

$$H\ddot{x} + C\dot{x} = \tau \quad (1)$$

where $H(x) = \{H_i(x_i)\}$ is the inertia of the system, $C(x, \dot{x}) = \{C_i(x_i, \dot{x}_i)\}$ denotes the Coriolis and centripetal forces, $\dot{H}(x) - 2C(x, \dot{x})$ is skew-symmetric, $x = \{x_i\}$ denotes the position coordinate, and $\tau = \{\tau_i\}$ denotes the input torque. Define a position error as $e = x^d - x$, where x^d denotes the desired position.

The position synchronization error seeks the difference amongst the position errors of the multiple axes, and is determined based on the synchronization function that actually defines the task (Sun and Mills, 2002). As in the work by Sun (2003), the synchronization goal $e_1 = e_2 = \dots = e_n$ is used in this paper, where e_i denotes the position error of each axis- i . Moreover, it might be more convenient or convincing that the synchronization errors are defined as differential position errors between each axis and its two adjacent axes in both directions, namely:

$$\begin{aligned} \varepsilon_1 &= 2e_1 - (e_2 + e_n) \\ \varepsilon_2 &= 2e_2 - (e_3 + e_1) \\ &\vdots \\ \varepsilon_i &= 2e_i - (e_{i+1} + e_{i-1}) \\ &\vdots \\ \varepsilon_n &= 2e_n - (e_1 + e_{n-1}) \end{aligned} \quad (2)$$

where ε_i denotes the synchronization error of each axis- i . If all synchronization errors in (2) are zero, the synchronization goal $e_1 = e_2 = \dots = e_n$ is achieved automatically. Compared to the work by Sun (2003), such definitions are more strict because the differential position errors in two directions are considered. Rewrite (2) in the matrix format:

$$\begin{bmatrix} \varepsilon_1 \\ \varepsilon_2 \\ \vdots \\ \varepsilon_{n-1} \\ \varepsilon_n \end{bmatrix} = \begin{bmatrix} 2 & -1 & 0 & \cdots & -1 \\ -1 & 2 & -1 & \cdots & 0 \\ \vdots & \ddots & \ddots & \ddots & \vdots \\ 0 & \cdots & -1 & 2 & -1 \\ -1 & 0 & \cdots & -1 & 2 \end{bmatrix} \begin{bmatrix} e_1 \\ e_2 \\ \vdots \\ e_{n-1} \\ e_n \end{bmatrix}, \text{ or,}$$

$$\varepsilon = T e \quad (3)$$

where $\varepsilon = [\varepsilon_1, \varepsilon_2, \dots, \varepsilon_n]^T$, $e = [e_1, e_2, \dots, e_n]^T$, and T denotes the synchronization transformation matrix and satisfies $T = T^T$. Our focus is to design the controller to guarantee asymptotic convergence to zero of both the position error e and the synchronization error ε .

Introduce a concept named coupled position error, defined by

$$E = e + \alpha \varepsilon \quad (4)$$

where α is a control gain that is diagonal and positive definite. Substituting (3) into (4) yields

$$E = (I + \alpha T)e \quad (5)$$

where I is an unit matrix. Since T is symmetric, $(I + \alpha T)$ is symmetric as well. If α is small enough, $(I + \alpha T)$ is positive definite and has full rank. On the other hand, α relates to the effect of the synchronization control. The higher the gain α , the more enhanced the synchronization control, which can be shown in the following experiments. Therefore, it should take balance in selection of α .

Obviously, $E \rightarrow 0$ implies $e \rightarrow 0$ and $\varepsilon \rightarrow 0$. Note that in the work by Sun (2003), the position and synchronization errors are not linearly coupled in the definition of the coupled position error, because of the use of integration of the synchronization error $\int \varepsilon dt$. As a result, convergence to zero of the coupled position error does not necessarily lead to convergence to zero of the synchronization error in the work by Sun (2003).

3. SET-POINT POSITION CONTROL

Firstly, a set-point position control is considered, in which the following conclusions hold:

$$\dot{e} = -\dot{x}, \quad \dot{\varepsilon} = T\dot{e} = -T\dot{x} \quad (6)$$

Design a PD-type synchronization control law in the following format:

$$\tau = K_p E + K_d \dot{E} + (I + \alpha T)^{-1} K_e \dot{e} \quad (7)$$

where K_p , K_d , and K_e are positive control gains. Substituting (7) into (1) yields:

$$H(x)\ddot{x} + C(x, \dot{x})\dot{x} = K_p E + K_d \dot{E} + (I + \alpha T)^{-1} K_e \dot{e} \quad (8)$$

Theorem 1. The proposed controller (7) guarantees $e \rightarrow 0$ and $\varepsilon \rightarrow 0$ as time $t \rightarrow \infty$, under the condition that the control gain K_e is large enough to satisfy $\lambda_{\min}\{K_e\} \geq \left\| \alpha T \left(\frac{1}{2} \dot{H}(x) - C(x, \dot{x}) \right) \right\|$, where $\lambda_{\min}\{K_e\}$ is the minimum eigenvalue of the gain matrix K_e .

Proof. Define a Lyapunov function candidate as

$$V = \frac{1}{2} \dot{e}^T (I + \alpha T) H(x) \dot{e} + \frac{1}{2} E^T K_p E \quad (9)$$

Here $(I + \alpha T)H(x)$ is positive definite since $(I + \alpha T)$ is positive definite when the control gain α is selected small enough, and $H(x) = \{H_i(x_i)\}$ is a diagonal positive definite matrix. Differentiating V with respect to time yields

$$\dot{V} = \dot{e}^T (I + \alpha T)H(x)\ddot{e} + \frac{1}{2}\dot{e}^T (I + \alpha T)\dot{H}\dot{e} + E^T K_p \dot{E} \quad (10)$$

Multiplying both sides of (8) by \dot{E}^T yields

$$\begin{aligned} & \dot{E}^T H(x)\ddot{x} + \dot{E}^T C(x, \dot{x})\dot{x} \\ & = \dot{E}^T K_p E + \dot{E}^T K_D \dot{E} + \dot{E}^T (I + \alpha T)^{-1} K_e \dot{e} \end{aligned} \quad (11)$$

Utilizing (5) and (6), rewrite (11) as

$$\begin{aligned} & -\dot{e}^T (I + \alpha T)H(x)\ddot{e} - \dot{e}^T (I + \alpha T)C(x, \dot{x})\dot{e} \\ & = \dot{E}^T K_p E + \dot{E}^T K_D \dot{E} + \dot{e}^T K_e \dot{e} \end{aligned} \quad (12)$$

Substituting (12) into (10) yields

$$\begin{aligned} \dot{V} & = \dot{e}^T (I + \alpha T) \left(\frac{1}{2} \dot{H}(x) - C(x, \dot{x}) \right) \dot{e} - \dot{E}^T K_D \dot{E} - \dot{e}^T K_e \dot{e} \\ & = -\dot{E}^T K_D \dot{E} - \dot{e}^T \left(K_e - \alpha T \left(\frac{1}{2} \dot{H}(x) - C(x, \dot{x}) \right) \right) \dot{e} \\ & \leq -\dot{E}^T K_D \dot{E} - \dot{e}^T \left(\lambda_{\min} \{K_e\} - \left\| \alpha T \left(\frac{1}{2} \dot{H}(x) - C(x, \dot{x}) \right) \right\| \right) \dot{e} \end{aligned} \quad (13)$$

Note that $e^T \left(\frac{1}{2} \dot{H}(x) - C(x, \dot{x}) \right) e = 0$ since

$$\left(\frac{1}{2} \dot{H}(x) - C(x, \dot{x}) \right) \text{ is skew symmetric. If the control gain } K_e \text{ is large enough to satisfy } \lambda_{\min} \{K_e\} \geq \left\| \alpha T \left(\frac{1}{2} \dot{H}(x) - C(x, \dot{x}) \right) \right\|, \text{ then } \dot{V} \leq 0.$$

Therefore, \dot{E} and \dot{e} are bounded in term of L_2 norm since they appear in \dot{V} . From (6) and (8), further conclude that \ddot{E} and \ddot{e} are bounded as well. Consequently, \dot{E} and \dot{e} are uniformly continuous, and thus from Barbalat's lemma, $\dot{E} \rightarrow 0$ and $\dot{e} \rightarrow 0$ as time $t \rightarrow \infty$. From (6), have $\dot{x} \rightarrow 0$ and $\ddot{x} \rightarrow 0$ as time $t \rightarrow \infty$. From the error dynamics (8), there exists an invariant set $\Psi = \{(x, \dot{x}) : \dot{x} = 0, E = 0, e = 0, \varepsilon = 0\}$. Therefore, LaSalle' theorem directly implies asymptotic stability of the system, i.e., $E \rightarrow 0$, $e \rightarrow 0$ and $\varepsilon \rightarrow 0$ as $t \rightarrow \infty$.

Theorem 1 holds provided that the condition $\lambda_{\min} \{K_e\} \geq \left\| \alpha T \left(\frac{1}{2} \dot{H}(x) - C(x, \dot{x}) \right) \right\|$ is satisfied. In practical implementation, it is not necessary to know H and C exactly to select K_e . Instead, the control gain K_e can be chosen highly enough (or α is small enough), so that the condition in Theorem 1 holds.

Although the control law (7) can be expressed as a PD error feedback control, i.e.,

$$\begin{aligned} \tau & = K_p (I + \alpha T)e + [K_D (I + \alpha T) + (I + \alpha T)^{-1} K_e] \dot{e} \\ & = \bar{K}_p e + \bar{K}_D \dot{e} \end{aligned} \quad (14)$$

it differs from the standard PD control in that the controller employs feedbacks of both position error e and coupled position error E to guarantee $E \rightarrow 0$ and $e \rightarrow 0$ simultaneously, and thus convergence of the synchronization error ε to zero is enhanced. As a result, satisfactory transient performance of synchronization can be ensured.

4. TRAJECTORY TRACKING CONTROL

The trajectory tracking control is considered now by adding feedforward control terms and a saturation function to the control law (7), namely,

$$\begin{aligned} \tau & = K_H \ddot{x}^d + K_C \dot{x}^d + K_p E + K_D \dot{E} + (I + \alpha T)^{-1} K_e \dot{e} \\ & \quad + \text{sign}(\dot{E}) K_N \end{aligned} \quad (15)$$

where K_H and K_C are positive feedforward control gains, and K_N is a parameter that satisfies

$$K_N = \Delta_H \|\ddot{x}^d\| + \Delta_C \|\dot{x}^d\| \quad (16)$$

in which Δ_H and Δ_C are scalars.

Two assumptions are introduced: i) x^d is bounded up to its second time derivative; and ii) $H(x)$ and $C(x, \dot{x})$ are bounded if their arguments are bounded. When $H(x)$ is time-varying, the second assumption holds locally, i.e., Coriolis and centripetal forces are bounded by the square of the velocity norm.

Substituting (15) into (1) yields the closed-loop dynamics:

$$\begin{aligned} H(x)\ddot{e} + C(x, \dot{x})\dot{e} + K_p E + K_D \dot{E} + (I + \alpha T)^{-1} K_e \dot{e} \\ + N + \text{sign}(\dot{E}) K_N = 0 \end{aligned} \quad (17)$$

where $N = (K_H - H(x))\ddot{x}^d + (K_C - C(x, \dot{x}))\dot{x}^d$, which is bounded.

Theorem 2. Considering a trajectory tracking problem from an initial position to a final position, the tracking controller (15) leads to $e \rightarrow 0$ and $\varepsilon \rightarrow 0$ as time $t \rightarrow \infty$, under the conditions:

1. The control gain K_e is large enough to satisfy

$$\lambda_{\min} \{K_e\} \geq \left\| \alpha T \left(\frac{1}{2} \dot{H}(x) - C(x, \dot{x}) \right) \right\|;$$

2. The scalars Δ_H and Δ_C are large enough to satisfy $\Delta_H \geq \|K_H - H(x)\|$ and $\Delta_C \geq \|K_C - C(x, \dot{x})\|$.

Proof. Define the same Lyapunov function candidate as in (9). Multiplying both sides of (17) by \dot{E}^T yields

$$\begin{aligned} \dot{E}^T H(x)\ddot{e} + \dot{E}^T C(x, \dot{x})\dot{e} + \dot{E}^T K_p E + \dot{E}^T K_D \dot{E} \\ + \dot{E}^T (I + \alpha T)^{-1} K_e \dot{e} + \dot{E}^T N + \|\dot{E}\| K_N = 0 \end{aligned} \quad (18)$$

Substituting (5) into (17) and then the resulting equation into (10) yields (19).

$$\begin{aligned}
\dot{V} &= \dot{e}^T (I + \alpha T) \left(\frac{1}{2} \dot{H}(x) - C(x, \dot{x}) \right) \dot{e} - \dot{E}^T K_D \dot{E} - \dot{e}^T K_e \dot{e} - \dot{E}^T N - \|\dot{E}^T\| K_N \\
&\leq -\dot{E}^T K_D \dot{E} - \dot{e}^T \left(K_e - \alpha T \left(\frac{1}{2} \dot{H}(x) - C(x, \dot{x}) \right) \right) \dot{e} + \|\dot{E}^T\| \cdot \|N\| - \|\dot{E}^T\| K_N \\
&\leq -\dot{E}^T K_D \dot{E} - \dot{e}^T \left(\lambda_{\min}\{K_e\} - \left\| \alpha T \left(\frac{1}{2} \dot{H}(x) - C(x, \dot{x}) \right) \right\| \right) \dot{e} - \|\dot{E}^T\| (K_N - \|N\|)
\end{aligned} \tag{19}$$

Under the condition $\lambda_{\min}\{K_e\} \geq \left\| \alpha T \left(\frac{1}{2} \dot{H}(x) - C(x, \dot{x}) \right) \right\|$, has

$$\dot{e}^T \left(\lambda_{\min}\{K_e\} - \left\| \alpha T \left(\frac{1}{2} \dot{H}(x) - C(x, \dot{x}) \right) \right\| \right) \dot{e} \geq 0.$$

Under the conditions $\Delta_H \geq \|K_H - H\|$ and $\Delta_C \geq \|K_C - C\|$, has

$$\begin{aligned}
&K_N - \|N\| = \Delta_H \|\ddot{x}^d\| + \Delta_C \|\dot{x}^d\| - \|N\| \\
&\geq \|K_H - H(x)\| \|\ddot{x}^d\| + \|K_C - C(x, \dot{x})\| \|\dot{x}^d\| - \|N\| \tag{20} \\
&\geq \|(K_H - H(x))\ddot{x}^d + (K_C - C(x, \dot{x}))\dot{x}^d\| - \|N\| = 0
\end{aligned}$$

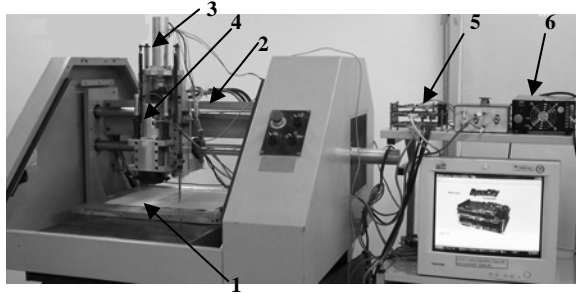
Therefore, $\dot{V} \leq 0$, and $\dot{E} \rightarrow 0$, $\dot{e} \rightarrow 0$ as time $t \rightarrow \infty$. The error dynamics (17) then becomes

$$K_p E + N = 0 \tag{21}$$

Since the desired velocity at the final position must be zero, have $\dot{x}^d = 0$ and $N = 0$ at the desired final position. Then have $E = 0$ from (21), and finally $e = 0$ and $\varepsilon = 0$. Using LaSalle's theorem, Theorem 2 can be finally proven.

5. EXPERIMENTS

A 4-axis experimental setup used to test the synchronization algorithms has been established as shown in Figure 1. A 4-axis motion control and driving integrated system (model no. DCT0040), supplied by DynaCity Technology (HK) Ltd, is used to control and amplify four DC brushless motors. The control application code is written in C and ASM language. A window utility program developed by Visual C++, enables us to quickly set up, configure, and troubleshoot controllers. The frequency of the position control loop is 4kHz.



1-Axis 1, 2- Axis 2, 3-Axis 3, 4-Axis 4, 5-Motion Control & Driving System, 6- Power Supply

Figure 1: Experimental setup

Firstly, the set-point position control was tested in driving four motors to rotate respectively one revolution (10000 counts) in a synchronous manner. The control gains are $K_p = \text{diag}\{1.1\}$, $K_D = \text{diag}\{0.1\}$, $\alpha = \text{diag}\{1\}$, and $K_e = \text{diag}\{0.1\}$. Figure 2 illustrates position and synchronization errors, respectively. It can be seen that besides good convergence of the position errors, there appears satisfactory performance in position synchronization. Figure 3 illustrates experimental results with the standard PD feedback control without synchronization, for comparison. Although position errors converge to zero eventually under the standard PD control, there appears worse transient performance of synchronization compared to that in Figure 2.

Secondly, the synchronous trajectory tracking controller was tested in controlling four motors to rotate respectively one revolution (10000 counts) in a synchronous manner along a trajectory specified as a cubic polynomial. The control gains for the trajectory tracking control are $K_p = \text{diag}\{1.1, 1.7, 1.1, 1.6\}$, $K_D = \text{diag}\{0.1\}$, $\alpha = \text{diag}\{1\}$, and $K_e = \text{diag}\{0.1\}$, $K_H = \text{diag}\{0.1\}$, $K_C = \text{diag}\{0.1\}$, $\Delta_H = \Delta_C = \text{diag}\{1\}$. Figures 4 and 5 illustrate the experimental results with the proposed synchronous tracking control and the standard PD control, respectively. Obviously, the synchronous control exhibits better synchronization performance.

The coupling parameter α plays important role in the synchronization. As α increases, the synchronization error decreases, but too large a value of α may affect the convergence speed of position errors. Figure 6 illustrates position and synchronization errors with different α ($\alpha = \text{diag}\{0.5\}$). Compared to Figure 4 where $\alpha = \text{diag}\{1\}$, it is seen that the use of smaller coupling parameter α results in smaller position errors but higher synchronization errors.

The robustness of the control law (15) to the unexpected disturbances in the motion is also tested, by adding a force disturbance to axis 3 at the time 40ms. Figure 7 shows that the added force disturbance does not produce large effect to the motion synchronization under the proposed synchronous control, since there is no obvious difference in the position synchronization compared to Figure 4. In contrast, under the standard PD control, the force disturbance degrades the

synchronization performance significantly, as can be seen in Figure 8.

6. CONCLUSIONS

In this paper, a model free cross-coupling controller is proposed for position synchronization of multi-axis motions. A PD-type cross-coupled controller is developed to asymptotically stabilize multi-axis motions while synchronizing positions of all axes in the set-point position control. The feedforward control terms and a saturation function can be further added to solve asymptotic trajectory tracking problem. The major advantage of the proposed method lies in its simplicity in implementation since it is model free and the control gains are not time-varying. Experimental results verify effectiveness of the proposed approaches.

REFERENCES

- Chiu, T. C., and Tomizuka, M. (2001). Contouring control of machine tool feed drive systems: A task coordinate frame approach, *IEEE Transactions on Control Systems Technology*, vol. 9, no. 1.
- Feng, L., Koren, Y., and Borenstein, J. (1993). Corss-coupling motion controller for mobile robots, *IEEE Control Systems*, 11, pp. 35-43.

- Koren, Y. (1980). Cross-coupled biaxial computer controls for manufacturing systems, *ASME Journal of Dynamic Systems, Measurement, and Control*, vol. 102, pp. 265-272.
- Koren, Y., and Lo C. C. (1991). Variable-gain cross-coupling controller for contouring, *Ann. CIRP*, vol. 40, no. 1, pp. 371-374.
- McNab R., and Tsao, T. (1994). Multiaxis contour tracking: A receding time horizon linear quadratic optimal control approach, *Dynamic System and Control*, vol. 2.
- Sun, D., and Mills, J. K. (2002). Adaptive synchronized control for coordination of multiple assembly tasks, *IEEE Trans. on Robotics and Automation*, vol. 18, no. 4, pp. 498-510.
- Sun D. (2003). Position synchronization of multiple motion axes with adaptive coupling control, *Automatica*, vol. 39, no. 6, pp. 997-1005.
- Tomizuha, M., Hu J. S., and Chiu, T. C. (1992). Synchronization of two motion control axes under adaptive feedforward control, *ASME Journal of Dynamic Systems, Measurement, and Control*, vol. 114, no. 2, pp. 196-203.
- Yeh, S., and Hsu, P. (1997). Theory and applications of the robust cross-coupled control design, *Proceedings of American Control Conference*.

APPENDIX: FIGURE 2~FIGURE 8

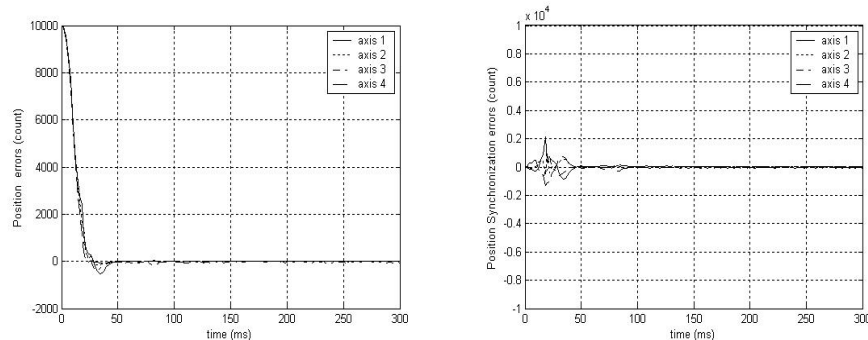


Figure 2: Results of the PD-based synchronization control in set-point control

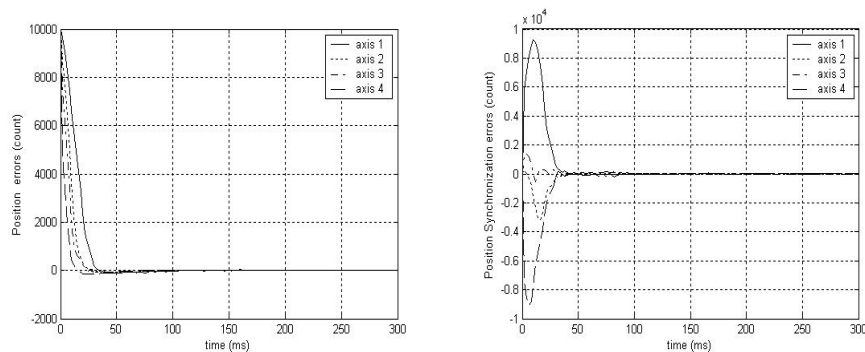


Figure 3: Results of standard PD control in set-point motion

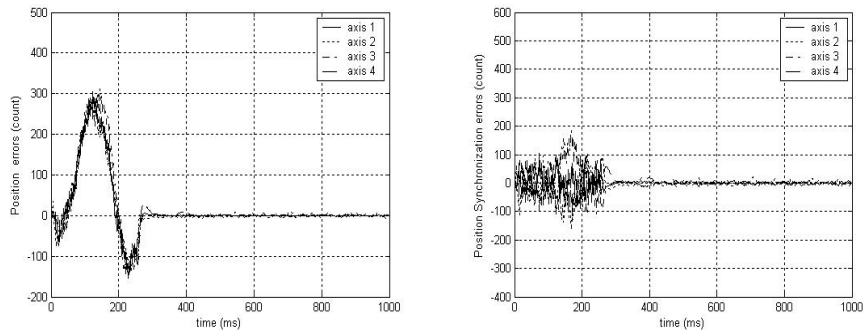


Figure 4: Results of synchronous tracking control

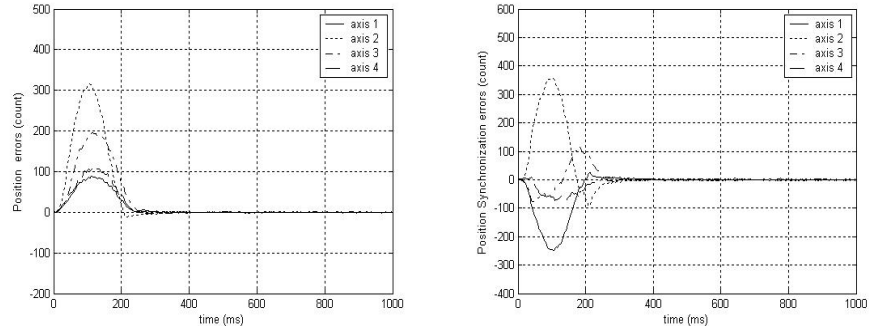


Figure 5: Results of standard PD control in trajectory tracking

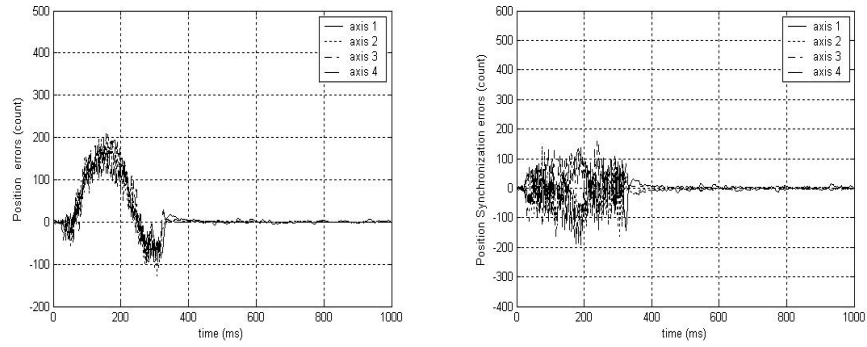


Figure 6: Results of synchronous tracking control ($\alpha = \text{diag}\{0.5\}$)

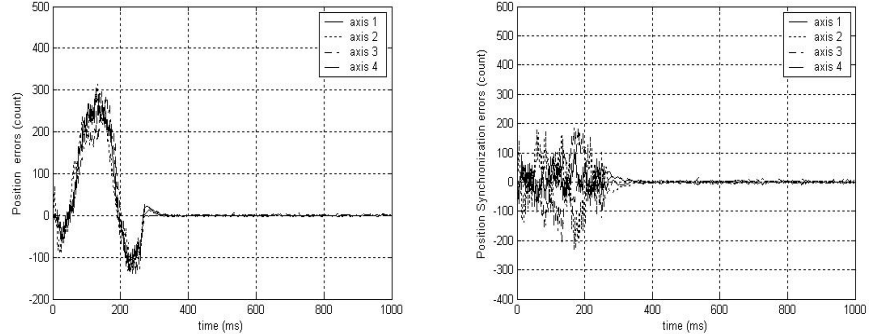


Figure 7: Results of synchronous tracking control with disturbance

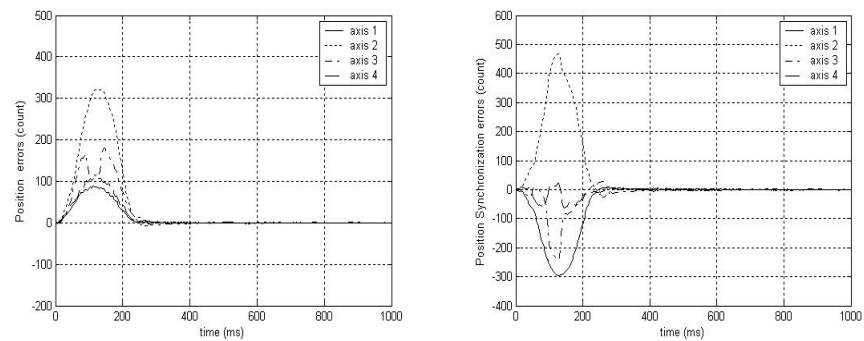


Figure 8: Results of the standard PD control with disturbance